Relevant Properties for Catalytic Activity of Sulfonic Ion-Exchange Resins in Etherification of Isobutene with Linear Primary Alcohols

Jordi Hug Badia, Carles Fité*, Roger Bringué, Eliana Ramírez, Montserrat Iborra

Chemical Engineering Department, Faculty of Chemistry, University of Barcelona, Martí i Franquès 1-11, 08028 Barcelona, Spain

* Corresponding author

E-mail addresses: jhbadia@ub.edu (J.H. Badia), fite@ub.edu (C. Fité), bringue@ub.edu (R. Bringué), eliana.ramirez-rangel@ub.edu (E. Ramírez), miborra@ub.edu (M. Iborra)

Abstract

The catalyzed liquid-phase reaction of isobutene with a homologous series of linear alcohols, from methanol to 1-butanol, has been studied at 333 K and 1.5 MPa. Sixteen sulfonic ion-exchange resins, to cover a wide range of properties, have been assayed. A response surface methodology analysis allowed to identify the most relevant catalyst properties, and the change of their relative importance along the homologous series of alcohols. Globally, reaction rates increase with the alcohol length. Resins with a high acid capacity and low specific volume of swollen polymer are the most active ones for the studied etherification reactions.

Keywords

alkyl tert-butyl ethers; isobutene; primary alcohol; sulfonic ion-exchange resins

1. Introduction

Methyl *tert*-butyl ether (MTBE) and ethyl *tert*-butyl ether (ETBE) have been produced in very large quantities in the last decades to be used as fuel components for gasoline engines. Progressively, ETBE has replaced MTBE production, because ETBE is environmentally more favorable. Both ethers are usually produced by addition of isobutene to methanol and ethanol under mild conditions, catalyzed by acidic ion-exchange resins. For ETBE, the use of bioethanol, obtained from plant sources, allows to qualify the obtained fuel as biofuel. Other ethers can be produced by means of the etherification of isobutene with larger alcohols, namely 1-propanol and 1-butanol, to obtain propyl *tert*-butyl ether (PTBE) and butyl *tert*-butyl ether (BTBE). An increase of the number of carbon atoms of the ether leads to a decrease in the vapor pressure and solubility in water, and to an increase in the boiling point [1,2]. These are desirable characteristics for gasoline blenders, because they allow a reduction of fuel evaporative emissions, a reduction of the risk of water contamination, and a dilution of harmful fuel components, like aromatics, what might help to fulfill more restrictive environmental legislation requirements of fuels in the future. Examples of these larger alcohols are 1-propanol or 1-butanol, which can be found as byproducts in a variety of natural fermentation processes. Industrially, these alcohols are produced mainly by means of the oxo process [3]. It consists of a selective hydroformylation and hydrogenation of linear olefins from fluid catalytic cracking in the presence of rhodium and cobalt phosphines [4,5]. Alternative routes for producing larger alcohols from biomass are the Guerbet catalysis process (condensation of bioethanol and/or biomethanol), and the ABE fermentation (which produces acetone, 1-butanol and ethanol using microorganisms of the genus *Clostridium*) [6,7]. Ethers from larger alcohols can be considered as promising oxygenates to be blended into gasoline, because they can be obtained from biomass and, therefore, they can be qualified as biofuels.

A number of works that studied the etherification of olefins with alcohols of a different number of carbon atoms can be found in the literature, where ion-exchange resins were used as catalysts [8–14]. Many of these studies focused on the reactivity of one olefin with one alcohol, while

others compared the behavior of various alcohols to draw conclusions on the reaction mechanism and the effect of reactant properties on the etherification. None of these works focused on the catalytic performance of the ion-exchange resins they used. In the present work, sixteen different ion-exchange resins have been assayed to compare their performance in the reactions to produce an analogous series of ethers and to relate the catalytic activity to the resin properties. Given the large number of properties and characteristics of these catalysts often found in literature, it is of interest to distinguish which ones have an actual relation with the resin catalytic performance.

2. Experimental

2.1. Chemicals

Reactants were methanol (max. water content 0.005% wt.), ethanol (max. water content 0.02% wt.), 1-propanol (max. water content 0.005% wt.), 1-butanol (max. water content 0.005% wt.), and a synthetic C_4 mixture as the 2-methylpropene (isobutene) source. A C_4 mixture containing 25% wt. of isobutene, 40% wt. of isobutane and 35% wt. of *trans*-2-butene was used as the isobutene source to approach an industrial C_4–cut stream. Methanol and ethanol were supplied by Panreac (Castellar del Vallès, Spain), 1-propanol and 1-butanol were supplied by Sigma-Aldrich (Tres Cantos, Spain) and the C_4 mixture was supplied by Abelló-Linde (Barcelona, Spain).

2.2. Catalysts

A total of sixteen ion exchange resins were used as catalysts, which are listed in Table 1 with their most relevant properties. They were all sulfonated macroreticular polymers with a styrene-divinylbenzene backbone. Twelve resins are commercially available, supplied by Rohm & Hass (Amberlyst™ type) and by Purolite®, and four had been produced in the lab (named as 306, 406, 606, and 806 [15]). They present a wide range of the properties of interest: acid capacity (from 0.8 to 5.6 meq H^+ / g_{cat}); crosslinking degree (low, medium, and high); sulfonation type (conventionally sulfonated –about one sulfonic group per benzene ring–,

oversulfonated –more than one sulfonic group per benzene ring–, partially sulfonated –less than one sulfonic group per benzene ring–, and surface sulfonated – sulfonated mainly on the surface of their microspheres). Among partially sulfonated resins, local differences in sulfur concentration within the beads have been reported in resins A46, 306, and 406 [15], and therefore they are considered to be sulfonated mainly on the surface of their microspheres. In the case of A70, in its manufacture some hydrogen atoms of the polymer chain are substituted by chlorine atoms to increase the thermal stability of the resin. This variety of properties was chosen to cover a wide range of morphological and chemical features to allow identifying which are relevant to the catalytic activity.

Table 1. Basic properties of ion-exchange resins used in this work

Catalyst	Short name	Acid Capacity, $[H^+]$ [a] [meq H^+ / g_{cat}]	%DVB [b]	Sulfonation type [c]
Amberlyst™ 15	A15	4.81	High	C
Amberlyst™ 16	A16	4.80	Medium	C
Amberlyst™ 35	A35	5.32	High	O
Amberlyst™ 36	A36	5.40	Medium	O
Amberlyst™ 39	A39	4.81	Low	C
Amberlyst™ 40	A40	5.01	High	O
Amberlyst™ 46	A46	0.87	High	S
Amberlyst™ 48	A48	5.62	High	O
Amberlyst™ 70 [d]	A70	2.65	Low	C
Purolite® CT175	CT175	4.98	High	C
Purolite® CT252	CT252	5.40	Medium	O
Purolite® CT275	CT275	5.20	High	O
306	306	0.81	High	S
406	406	0.99	High	S
606	606	1.89	High	P
806	806	3.10	High	P

[a] Titration against standard base. [b] %DVB: divinylbenzene amount. Cross-linking degree classification considered: Low (≤8%); Medium (9-14%); High (>14%).
[c] C: Conventionally sulfonated; O: Oversulfonated; S: Surface sulfonated; P: Partially sulfonated. [d] Amberlyst 70 is a chlorinated resin.

As it is well known, the resin lifespan in industrial operation for this type of reactions has been reported to be so long that it can last even years under mild conditions [16,17]. In this sense, previous experience from the authors revealed that, in the absence of catalyst killers, no significant activity loss was observed in a similar reaction system, the ETBE production catalyzed by CT275, after 115 h of time on stream, operating with a liquid hourly space velocity of 2 h^{-1} at 353 K and 1.5 MPa. Studies regarding the long durability of the same type of resins in

other reaction systems, such as dehydration reactions of either linear alcohols or fructose, can be found elsewhere [3,18].

Since catalysts were supplied in wet state, the resins pretreatment consisted in reducing their water content. Catalysts were firstly air-dried at room temperature for 48 h to remove the free water from the resin beads and, afterwards, introduced in an atmospheric oven during a minimum of 14 h at 383 K to remove the bounded water molecules. Catalysts were then kept in the oven until the experiment was carried out.

2.3. Apparatus and experimental procedure

The experimental setup consisted of a catalytic fixed bed tubular microreactor (length: 150 mm, i.d.: 7 mm) submerged in a thermostatic bath to maintain the reactor at the desired temperature. In order to get an isothermal reactor bed, catalyst was diluted with silicon carbide of the same particle size range. Silicon carbide had been proven to be inert in terms of reaction. If catalyst dilution were too large, flow deviations like preferential paths or by-passing effects could arise. In a previous work [19], it was found that an inert/catalyst mass ratio up to 300 did not affect the kinetic results for the present system. Therefore, dilution was kept under that value for all the experimental runs.

Experiments were carried out at 333 K. Reactor feed was free of product, what means null isobutene conversion level at the reactor inlet. Alcohol/olefin molar ratio ($R^{o}_{A/O}$) at the reactor inlet was set to 1.0. Firstly, only alcohol was fed, similarly to the reactor startup procedure at industrial scale, and then the reactor was submerged in the thermostatic bath. The aim of this procedure is to heat up the catalyst bed and to reduce, as much as possible, the remaining water in the catalyst by alcohol percolation. As seen in previous works, when an alcohol volume of more than 10 times the catalytic bed volume is passed through the bed, the water content in the resin can be considered lower than 1%wt. [20]. Afterwards, while the alcohol flow was kept constant, the C_4 mixture was added to the reactor feed for the reaction to proceed. Around 3-4 h

were needed for each kinetic run to reach the steady state. This fact was verified by repeated chromatographic analysis at the reactor outlet.

2.4. Chemical analysis

Along every experimental run, samples of the reaction medium were taken inline from the reactor inlet and outlet streams through two sampling valves that injected 0.2 μL of pressurized liquid into an Agilent gas chromatograph 7890A (Santa Clara, US) equipped with a capillary column HP-PONA 19091S-001 (100% dimethylpolysiloxane, 50 m × 0.20 mm × 0.50 μm; J&W Scientific, Santa Clara, US). Hydrogen (minimum purity of 99.9995%; Air Liquide, Barcelona, Spain) and synthetic air (minimum purity of 99.999%; Air Liquide, Barcelona, Spain) were used for the FID detector. Helium (minimum purity of 99.998%; Abelló-Linde, Barcelona, Spain) was used as the carrier gas with a flow of 0.75 mL / min. Oven temperature ranged from 308 to 343 K depending on the considered reaction. This analytical system allowed identifying and quantifying the reactants, the inert components of the C_4 mixture, the formed ether and the reaction byproducts, when formed.

2.5. Calculations

Reaction rates were calculated from isobutene consumption in the reactor at steady state, since no side reactions were detected. For a plug-flow fixed bed catalytic reactor under differential regime, the following expression applies:

Reaction rate: $$-r_{IB} = F^{o}_{IB}\left(X_{IB,outlet} - X_{IB,inlet}\right)\Big/W_{cat} \quad (1)$$

where F^{o}_{IB} is the isobutene reference molar flow at null conversion, $X_{IB,outlet}$ is the isobutene conversion at the reactor outlet, $X_{IB,inlet}$, the inlet isobutene conversion, was zero, and W_{cat} is the catalyst mass in dry basis.

Relative conversion: $$X_{IB} = 1 - F_{IB,outlet}\,/\,F_{IB,inlet} \quad (2)$$

In order to provide an empirical relationship between catalysts properties and reaction rates, a response surface methodology analysis was carried out by means of the stepwise procedure and considering a second-order polynomial expression with interaction terms, as follows:

$$y = \beta_0 + \sum_{i=1}^{k} \beta_i x_i + \sum_{i=1}^{k} \beta_{ii} x_i^2 + \sum \sum_{i<j=1}^{k} \beta_{ij} x_i x_j \quad (3)$$

where y is the response variable, x the independent variables, and β the equation coefficients.

3. Results and discussion

3.1. Reaction system

Given that methyl *tert*-butyl ether and ethyl *tert*-butyl ether syntheses are chemical processes of industrial interest that have been widely studied [21–24], a series of analogous reactions is proposed. These reactions are the alkyl *tert*-butyl ether syntheses from isobutene and linear primary alcohols with one to four carbon atoms. Alkyl *tert*-butyl ethers are formed by addition of the corresponding alcohol to isobutene (IB). Methanol (MeOH), ethanol (EtOH), 1-propanol (1-PrOH), or 1-butanol (1-BuOH) were used to obtain, respectively, methyl *tert*-butyl ether (MTBE), ethyl *tert*-butyl ether (ETBE), propyl *tert*-butyl ether (PTBE), or butyl *tert*-butyl ether (BTBE) (Fig.1). Kinetic data from the first two well-known reactions can also be used as a reference to validate the data obtained for the other two less-known reactions.

FIGURE 1

This type of reactions can be explained by a mechanism that consists of a series of elementary steps. Firstly, reactants adsorb on the resin active sites, then the surface reaction between the adsorbed alcohol and isobutene (either adsorbed or from the liquid solution) follows to form a molecule of adsorbed ether, which finally desorbs [25,26] (Fig.2). It can be considered that the reactions to form each ether proceed through a similar mechanism, since the only difference is the number of carbon atoms in the alcohol chain.

FIGURE 2

Possible side reactions comprise isobutene dimerization to form 2,4,4-trimethyl-1-pentene and 2,4,4-trimethyl-2-pentene, isobutene hydration to form *tert*-butyl alcohol, alcohol dehydration to form the corresponding symmetric ether and water, and etherification of 2-butene from the synthetic C_4 mixture with alcohol to form the corresponding alkyl *sec*-butyl ether. Byproducts formation was avoided (less than 0.3% GC) by setting a relatively low temperature (333 K) and the stoichiometric initial molar ratio alcohol/olefin ($R^o_{A/O}$ = 1.0). These conditions are known to minimize side-reactions according to literature data on the present reaction systems and similar ones [27–30]. In particular, byproducts formation can be dismissed in the present work, because the relative difference of the molar carbon balance applied to every experimental point by considering only the etherification reaction was always below 2%.

3.2. Preliminary experiments

To evaluate reaction rates as a basis of the composition change between reactor inlet and outlet using Eq. 1, the reactor needs to operate under differential regime, where the reaction rate can be considered constant along the reactor. For both MTBE and ETBE systems, literature data showed that the reactor behaves differentially when the isobutene conversion is at least below 10% [24,31]. This value has been confirmed experimentally also for PTBE and BTBE systems, as seen in Fig.3. Accordingly, the mass of catalyst in the experiments was chosen to obtain up to around a 10% isobutene conversion values at 333 K.

FIGURE 3

With respect to the external mass transfer influence, experiments were carried out at different flow rate values, characterized by the weight hourly space velocity (WHSV), in the four considered reaction systems for a choice of catalysts. Selected resins cover the whole range of catalysts properties. As Fig. 4a and 4b show, the external mass transport influence can be

neglected at least for WHSV higher than 500 h^{-1} at 333 K, which corresponds to a linear velocity higher than 0.17 cm/s calculated for empty tube.

FIGURE 4

To check if internal mass transfer effects are present, due to the diffusion of species within the resin backbone, reaction rates were measured using different resin bead sizes. These effects would become more apparent with bigger molecular size of involved species, and larger particles for a catalyst with relatively small pore volume, resulting in a measured reaction rate lower than without diffusional effects. To cover the wide range of pore volume, experiments for both PTBE and BTBE synthesis reactions were carried out with CT275 and A39, which present the largest and the smallest pore volumes, respectively, among the assayed catalysts. As seen in Fig. 5, internal mass transport effects can be considered as negligible within the experimental error at 333 K and $R^{o}_{A/O} = 1.0$ for all assayed bead sizes. Since the involved molecules in the MTBE and ETBE reaction systems are smaller, mass transfer effects are expected to be non-significant under the same experimental conditions. Therefore, in a conservative manner, all further experiments with every catalyst were carried out with particle diameter smaller than 0.40 mm to avoid diffusional effects.

FIGURE 5

3.3. Effect of the linear primary alcohol

Table 2 lists the experimental reaction rates obtained for the four considered reactions with each catalyst. As seen, in the experiments with more active catalysts (A15, A35, A36, A40, A48, CT175, CT252, and CT275), reaction rates followed the order 1-butanol > 1-propanol > ethanol > methanol, as already described in literature [8]. But with less active catalysts (A16, A39, A46, A70, 306, 406, 606, and 806), methanol was more reactive than ethanol. Replicated experiments allowed to estimate the uncertainty in reaction rates values, ranging from 0.5% to 7.0%, and

mainly below 2.2%, which is an acceptable level of experimental error. The uncertainty of the non-replicated experiments can be assumed to be of the same order.

Table 2. Isobutene consumption rates for alkyl *tert*-butyl ethers, with the estimated standard error for replicated experiments. T = 333 K, $R^{o}_{A/O}$ = 1.0, d_p = 0.25-0.40 mm, WHSV > 500 h^{-1}

Catalyst	$-r_{IB}$ [mol $(g_{cat}\ h)^{-1}$]			
	MTBE	**ETBE**	**PTBE**	**BTBE**
A15	0.098 ± 0.002	0.117	0.275	
A16	0.0951 ± 0.0017	0.0812	0.211	0.457
A35	0.135 ± 0.002	0.1624 ± 0.0002	0.529 ± 0.012	1.228
A36	0.136	0.140		
A39	0.0766 ± 0.0005	0.057 ± 0.004	0.113 ± 0.004	0.191 ± 0.011
A40	0.109	0.126		
A46	0.0076 ± 0.0005	0.0061	0.0082	0.0186
A48	0.135	0.152		
A70	0.0393	0.0240	0.0414	0.0596
CT175	0.101	0.126		
CT252	0.114	0.118		
CT275	0.125	0.133	0.379 ± 0.008	0.795 ± 0.011
306	0.0058	0.0052	0.0064	0.0119
406	0.0084	0.0058	0.0089	0.0160
606	0.01982 ± 0.00013	0.0158	0.0328	0.0583
806	0.0432	0.0380	0.0980	0.204

In a first approach, for a given catalyst the observed reactivity variation can be attributed to the different used alcohols, whose main properties are shown in Table 3.

Table 3. Alcohols properties

Alcohol	Number of Carbon Atoms	Molar Weight [g mol^{-1}]	Molar Volume [cm^3 mol^{-1}] [a]	Molecular Length [nm] [b]	Dipole Moment [D] [c]	pK_a [d]	Hildebrand Solubility Parameter, δ_j [$MPa^{1/2}$] [e]
MeOH	1	32.04	42.10	0.30	1.700	15.09	27.9
EtOH	2	46.07	60.20	0.41	1.691	15.93	25.2
1-PrOH	3	60.10	77.64	0.55	1.679	16.10	23.4
1-BuOH	4	74.12	94.28	0.66	1.661	16.10	21.8

[a] Estimated by the Hankinson-Brobst-Thomson (HBT) method at 1.5 MPa and 333 K [32,33]. [b] Calculated from the distances and angles of bonds between atoms using ChemBioOffice 2013 software, for minimum energy conformation. [c] From [34]. [d] From [35]. [e] Estimated at 1.5 MPa and 333 K according to [32,33]

From values in Table 3, it can be observed that some alcohol properties are correlated with the alcohol length. In this sense, alcohols molar weight, volume, and length increase proportionally with their number of carbon atoms. In contrast, dipole moment and Hildebrand solubility parameter diminish in different manner as the number of carbon atoms increases, while pK_a

hardly changes. Isobutene reaction rate for the tested catalysts in the four reaction systems is plotted as a function of the alcohol number of carbon atoms in Fig. 6.

FIGURE 6

Globally, from Fig. 6, isobutene reacts faster with larger alcohols: BTBE formation is the fastest reaction, and, on average, PTBE formation is about the half, and ETBE and MTBE formation, both similar, are about the third. With regard to the reaction rate variation as a function of the other properties listed in Table 3, similar figures can be obtained. For instance, reaction rates increase with decreasing alcohol polarity and increasing pK_a.

The effect of the alcohol polarity on reaction rates can be explained by the ease of more polar compounds to swell the resin backbone and to solvate the acidic protons of the sulfonic groups by breaking the hydrogen bond network. Then, although more catalytic centers become accessible to reactants by the swelling effect, the proton donor-acceptor strength of these centers is reduced by the protons solvation, with a result of lower reaction rates [9,24,36–39]. As for the effect of the alcohol pK_a, larger alcohols present, as a general rule, less acidity (Table 3). As it is known, alcohols undergo protonation in the presence of acids. Less acidic alcohols can protonate easier with the resin sulfonic acid groups than more acidic alcohols. This fact can explain the faster reaction rates displayed by larger alcohols given that the protonation of the alcohol is considered to be included in the etherification reaction mechanism [8,9].

On the other hand, rates generally increase for alcohols presenting lower values of the Hildebrand solubility parameter, δ. This parameter accounts for the interaction between the liquid mixture and the resin: compounds with similar values of δ are likely to present higher affinity. Thus, alcohols presenting a high affinity for a resin can permeate easier into it and reach a larger number of active sites, what would contribute to enhance reaction rates. The Hildebrand solubility parameter of each used resin, δ_P, can be estimated at 298 K by a group contribution method [40], their values ranging 22.4-25.6 $MPa^{1/2}$ (Table 4), by means of the following expression:

$$\delta_P = \sqrt{\frac{\sum_i x_i E_{coh,i}}{\sum_i x_i V_i}} \quad (4)$$

In Eq. 4, x_i, $E_{coh,i}$, and V_i are, respectively, the molar fraction, the cohesion energy and the molar volume of each structural group *i* present in the resin. At the operating temperature of 333 K, δ_P values are expected to either remain constant or to slightly decrease in comparison to those in Table 4 [41]. The value of δ presented by ethanol, δ_{EtOH}, is globally closer to the δ_P values presented by most resins, with some exceptions: resins A46, 306, and 406 present δ_P values closer to $\delta_{1\text{-}BuOH}$, and A70, 606, and 806 present δ_P values closer to $\delta_{1\text{-}PrOH}$. This fact would be related to the ease of permeation of these alcohols into the catalyst backbone in the mentioned cases.

Table 4. Estimated values of Hildebrand solubility parameter at 298 K for the assayed catalysts

Catalyst	δ_P [MPa$^{1/2}$][a]
A15	24.9
A16	24.7
A35	25.4
A36	25.2
A39	24.6
A40	25.1
A46	22.4
A48	25.6
A70	23.2
CT175	25.0
CT252	25.2
CT275	25.2
306	22.4
406	22.5
606	22.9
806	23.6

[a] Estimated at 298 K [40]

In the reaction medium, alcohols only represent a relatively small proportion of the reactive liquid mixture in contact with the resin. Then, if Hildebrand solubility parameters of the mixture, δ_M, are used instead of δ for each alcohol, their differences with δ_P values are much higher: mean δ_M values were 13.287 ± 0.001, 13.271 ± 0.007, 13.75 ± 0.02, and 13.53 ± 0.04 MPa$^{1/2}$ for the reacting mixture in the MTBE, ETBE, PTBE, and BTBE systems, respectively. As seen in Fig. 7, (δ_P – δ_M) difference values in the syntheses involving 1-propanol and

1-butanol are globally slightly smaller than when involving methanol and ethanol. This fact would be related to the observed reactivity gradation.

FIGURE 7

Fig. 7 shows a similar trend of the isobutene consumption rate with respect to ($\delta_P - \delta_M$) difference for every reaction system. This fact supports that the affinity between the resin and the reaction medium would affect similarly the catalytic activity for different reaction systems.

3.4. Relation between resins properties and catalytic activity

As seen in both Fig. 6 and Fig. 7, the relative reactivity of a given resin compared to the others hardly changes irrespectively of the alcohol, what would indicate a relation between the resin morphological properties and its activity.

Acid capacity is often found in literature for some acid-catalyzed reactions as a key factor of the catalytic activity of a resin, e.g., [8]. In this sense, Fig. 8 plots reaction rate against resins acid capacity, which shows that reaction rates globally increase as acid capacity increases. This trend becomes less clear for highly acidic resins (>4.8 meqH^+/g_{cat}). It has been stated that high sulfonic groups concentration can also have a counter effect regarding accessibility of reactants towards active sites because of steric hindrances [36], what could lower their overall efficiency per active center. As a conclusion, it seems that the acid capacity is not the only determining factor to explain catalyst activity differences.

FIGURE 8

Previous investigations on several reaction systems have indicated that the catalytic activity of a given resin is determined by its capacity and morphological properties, in both dry and water-swollen state [3,15,42–45]. To identify the key catalytic features in its performance, all basic properties (Table 1) and morphological properties (Table 5) of the assayed resins have been analyzed, and an empirical model is proposed to predict reaction rates as a function of the relevant catalyst properties. Dry-state characteristics include the BET (Brunauer-Emmett-Teller)

surface area (S_{BET}), the BJH (Barrett-Joyner-Halenda) desorption cumulative surface area (S_g) and volume (V_g) of pores, and the mean pore size ($d_{p,m}$). The considered water-swollen state characteristics were the surface area (S_{area}), volume (V_{pore}) and size (d_{pore}) of meso-macropores, as well as the specific volume of swollen polymer (V_{sp}), which corresponds to the micropore-size cavities in the resins gel-phase. The water-swollen state values were obtained by the Inverse Steric Exclusion Chromatography (ISEC) technique, which characterizes the swollen polymer to provide information on pore volume distributions [46–48]. On the other hand, resins characterization by means of other well-known techniques, such as scanning electron microscopy or spectroscopy [49,50] , would not reveal significant information, because all the tested catalysts are composed of sulfonic groups as active sites placed on a macroreticular styrene-divinylbenzene backbone, with a typical cauliflower-like appearance of the internal pore structure [51,52].

Table 5. Morphological properties of the tested resins both in dry and in water-swollen state

Catalyst	ρ [a] [g · cm^3]	Dry state: adsorption-desorption of N_2 at 77 K [b]				Swollen in water (ISEC method)			
						Macro-mesopores			Gel phase
		S_{BET} [c] [m^2 g^{-1}]	S_g [m^2 g^{-1}]	V_g [d] [cm^3 g^{-1}]	$d_{m,pore}$ [e] [nm]	S_{area} [m^2 g^{-1}]	V_{pore} [cm^3 g^{-1}]	d_{pore} [e] [nm]	V_{sp} [cm^3 g^{-1}]
A15	1.416	42.0	41.3	0.328	31.8	192	0.616	12.8	0.765
A16	1.401	1.69	1.75	0.013	29.7	46.2	0.188	16.3	1.129
A35	1.542	29.0	35.6	0.210	23.7	199	0.720	14.5	0.613
A36	1.567	21.0	21.2	0.143	27.0	68.0	0.259	15.2	1.025
A39	1.417	0.09	0.065	0.0003	17.6	56.1	0.155	11.1	1.624
A40	1.431	0.22	0.32	0.0006	7.5	11.0	0.125	45.5	0.442
A46	1.137	57.4	54.8	0.263	19.2	186	0.470	10.1	0.523
A48	1.538	33.8	32.1	0.249	31.0	186	0.568	12.2	0.620
A70	1.514	0.018				66.1	0.220	13.3	1.257
CT175	1.498	28.0	26.6	0.30	45.1	90.7	0.615	27.1	0.908
CT252	1.493	22.4	19.9	0.221	44.4	132	0.491	14.9	0.981
CT275	1.506	20.3	30.2	0.377	50.1	209	0.772	14.7	0.806
306	1.112	38.1	40.6	0.267	26.4	156	0.408	10.5	1.247
406	1.129	35.8	39.6	0.272	27.5	136	0.643	18.9	0.934
606	1.177	30.4	33.5	0.233	27.8	122	0.652	21.3	0.951
806	1.263	26.5	29.0	0.198	28.0	62.2	0.455	29.3	1.250

[a] Skeletal density. Measured by helium displacement (Accupic 1330). [b] Samples dried at vacuum (0.001 MPa, 383 K). [c] BET method. [d] Volume of N_2 adsorbed at relative pressure (P/P_0) = 0.99. [e] $d_{m,pore} = 4V_g/S_g$ or $d_{pore} = 4V_{pore}/S_{area}$, respectively.

A response surface methodology analysis has been used to find the most significant factors that explain reaction rate variability in terms of resins properties for each reaction system. The searched model consists of an expression with the lowest number of terms in which all

parameters and the regression itself are statistically significant within a 95% confidence level. Independent variables were coded each to fit the range -1 to +1. The best empirical model for each reaction was searched among second order polynomials with interaction terms by means of the stepwise procedure. As polynomials are empirical models, square roots of etherification rates, rather than actual rates, were used as response variable, because they provided a better fit, and residuals followed more closely a normal distribution. Table 6 lists the parameter values, with their standard error and *p*-value, the regression F statistic, and the adjusted R^2 for the resulting best empirical model for each reaction system using coded regressors.

Table 6. Data analysis for coded regressors

Reaction		Term				F_{reg}	$R^2_{adjusted}$
		β_0	β_1 ($[H^+]$)	β_2 (V_{sp})	β_{12} [a] ($[H^+]\cdot V_{sp}$)		
MTBE	Coefficient	0.219	0.141	–0.016	–	577.9	0.987
	p-value	<0.0001	<0.0001	0.0195	–		
	St. Error	0.003	0.004	0.006	–		
ETBE	Coefficient	0.212	0.147	–0.038	–0.029	261.7	0.981
	p-value	<0.0001	<0.0001	0.0013	0.0343		
	St. Error	0.005	0.006	0.009	0.012		
PTBE	Coefficient	0.328	0.259	–0.104	–0.101	169.7	0.981
	p-value	<0.0001	<0.0001	0.0008	0.0046		
	St. Error	0.009	0.014	0.018	0.025		
BTBE	Coefficient	0.477	0.390	–0.200	–0.173	129.3	0.977
	p-value	<0.0001	<0.0001	0.0007	0.0059		
	St. Error	0.017	0.024	0.032	0.041		

[a] The ($[H^+]\cdot V_{sp}$) term was statistically non-significant for the MTBE system

According to the analysis results, reaction rates depend on the same two resin properties, irrespectively of the considered reaction system: the acid capacity, $[H^+]$, and the specific volume of swollen polymer, V_{sp}. Results suggest a linear effect of $[H^+]$ and V_{sp} on $\sqrt{-r_{IB}}$ in every reaction system, and also an interaction effect of $[H^+]\cdot V_{sp}$, except for MTBE, where the interaction term was non-significant. Any other resin property effect was found to be statistically non-significant. Table 6 shows that each fitted parameter presents the same sign in every reaction system, and therefore the related property has a similar effect on the reaction rate. For instance, since β_1 is positive, $[H^+]$ enhances reaction rate, and negative values of β_2 and β_{12} indicate that both V_{sp} and the interaction term $[H^+]\cdot V_{sp}$ have a negative effect on reaction rates. Moreover, the relative importance of regressors in each reaction system has been assessed to

determine the relative effect of each term [53]. Results, plotted in Fig. 9, show that $[H^+]$ is by far the factor with the highest relative impact, and it gradually loses weight as the alcohol size increases. In contrast, V_{sp} and the interaction term $[H^+]\cdot V_{sp}$ have a very low effect on reaction rate in the MTBE system, but their relative importance increases substantially with larger alcohols. This fact can be attributed to the relation of V_{sp} with the empty space between polymer chains of the resin, a factor that becomes more important for larger molecules.

FIGURE 9

The derived expressions, in terms of uncoded regressors, are:

MTBE: $$\sqrt{-r_{IB}} = +0.0592 + 0.0585\,[H^+] - 0.0272\,V_{sp} \quad (5)$$

ETBE: $$\sqrt{-r_{IB}} = +0.0124 + 0.0825\,[H^+] - 0.0023\,V_{sp} - 0.0206\,[H^+]\,V_{sp} \quad (6)$$

PTBE: $$\sqrt{-r_{IB}} = -0.0681 + 0.1796\,[H^+] + 0.0520\,V_{sp} - 0.0709\,[H^+]\,V_{sp} \quad (7)$$

BTBE: $$\sqrt{-r_{IB}} = -0.0981 + 0.2877\,[H^+] + 0.0531\,V_{sp} - 0.1217\,[H^+]\,V_{sp} \quad (8)$$

where $-r_{IB}$ is expressed in mol $(g_{cat}\ h)^{-1}$, $[H^+]$ in meqH^+ g_{cat}^{-1}, and V_{sp} in cm^3 mol^{-1}. Fig. 10 compares experimental and predicted reaction rates using Eq. 5 to 8, which shows a satisfactory fit over the whole range of reaction rate values.

FIGURE 10

As Fig. 11 illustrates, the shape of the response surface is similar for all considered reactions, with a progressively relative increasing effect on the reaction rate at low V_{sp} and high $[H^+]$ as a larger alcohol is used. On the other hand, the four response surfaces show very low reaction rate values and they are almost not sensitive to V_{sp} for resins with very low acid capacity (surface sulfonated resins 306, 406, and A46).

FIGURE 11

These models allow us to provide an explanation regarding the relation between the resins morphological properties and their activity. As expected, a high acid capacity, [H^+], favors etherification rates. As for the V_{sp}, a low value implies a more rigid structure, less swollen, when the resin is in the reaction medium. Such rigidity entailed faster rates and this effect is more accused for larger alcohols. From a catalyst manufacturer standpoint, this fact implies that maintaining a high active site local concentration in the gel phase and preventing an excessive swelling of the polymer backbone contributes to reach higher reaction rates. On the other hand, in regard to the reaction medium properties variation, present results point out that the reaction of isobutene with larger alcohols is more affected by the spatial conformation, with some relative reduction of the importance of the acid capacity of the catalysts by itself.

Since all reactants present a sufficiently low molecular size, it is not expected that important steric hindrances arise when they permeate through the resin network [54]. Consequently, a larger network flexibility would not enhance etherification rates by easing reactants transport through it. On the contrary, it would reduce the local concentration of active sites per unit volume by the increase of the distance between them. Therefore, a high acidity is desirable, so the reactants can be coordinated to multiple active sites to form products readily, what can lead to higher reaction rates.

Given that acid capacity and specific swollen polymer volume are able to explain most of the observed reaction rate variation, a combination of such properties could contribute to simplify the understanding of their joint effect. For instance, if the ratio [H^+]/V_{sp} is considered, which would be related to the active sites concentration in the gel phase [44], a clear trend of the etherification rate, similar for all reaction systems, is observed (Fig. 12).

FIGURE 12

Two well defined regions can be observed in Fig. 12. At low [H^+]/V_{sp} (< 2 meqH^+ cm^{-3}, characteristic of the partially sulfonated resins 306, 406, A46, and 606) all reactions present very low and similar reaction rate values, probably due to a low amount of adsorbed species on

the resins and to a large distance between adjacent active sites. At high $[H^+]/V_{sp}$ (> 2 meqH^+ cm^{-3}), reaction rates increase, attributable to a better coordination of reactant molecules with the active sites, because of the higher concentration of active sites in the gel phase. This reaction rate enhancement is sharper for reactions involving larger alcohols, what supports the idea that the studied reactants do not present steric hindrances, but, on the contrary, reaction of isobutene with larger alcohols is favored by interactions between the resin backbone and the longer hydrocarbon chain of the alcohol. It is worth mentioning that the production of both MTBE and ETBE seems to become insensitive to the active sites concentration in the gel phase above $[H^+]/V_{sp} = 5$ meqH^+ cm^{-3}. To confirm this issue, more experimental data should be gathered for the whole series of the studied reactions.

Finally, cross-matching $[H^+]/V_{sp}$ values with data in Table 2, it is observed that the alcohols reactivity followed the order of the alcohols series 1-butanol > 1-propanol > ethanol > methanol for resins with high $[H^+]/V_{sp}$ (5.3–11.3 meqH^+ cm^{-3}), whereas methanol and ethanol swap their position for resins with low $[H^+]/V_{sp}$ (0.6–4.2 meqH^+ cm^{-3}). In this sense, methanol would be able to penetrate deeper than ethanol into the gel phase in resins with low density of active sites (i.e. low $[H^+]/V_{sp}$ values), probably due to its smaller size and, therefore, methanol would access to a large number of active sites than ethanol, with a result of faster reaction rate. On the other hand, methanol would not be able to penetrate any deeper than ethanol into the gel phase in resins with a higher density of active sites (i.e. higher $[H^+]/V_{sp}$ values). In this situation, reactants transport within the gel-phase would be driven only by interactions between the polymer backbone of the resin and the hydrocarbon chain of the alcohol.

4. Conclusions

The catalytic performance of ion-exchange resins in the addition of isobutene to a homologous series of four linear primary alcohols to obtain methyl (MTBE), ethyl (ETBE), propyl (PTBE) and butyl *tert*-butyl ether (BTBE) has been studied. Sixteen different ion-exchange resins have been assayed to cover a wide range of properties. Globally, etherification reactions rates present

an upward gradation as the alcohol is larger (1-butanol > 1-propanol > ethanol ~ methanol). The response surface methodology has been applied to the kinetic results for each reaction system to identify the catalyst properties that determine the catalytic activity. In all cases, they were the acid capacity and the specific volume of the swollen polymer gel phase. Acid capacity has been, by far, the most important property, and the specific volume of the swollen polymer gel phase gains weight progressively as the alcohol size increases. An empirical equation for each reaction system is provided that can explain satisfactorily the experimental reaction rate values, within a 95% confidence level. According to these models, highly-acidic resins with a rigid morphology are the most active catalysts in the present reaction systems.

Acknowledgements

The authors thank Rohm and Haas SAS France (The Dow Chemical Company) and Purolite Ltd. for supplying Amberlyst™ and Purolite® ion exchange resins, respectively, and to Dr. Karel Jeřábek for providing the ISEC analysis results.

This research did not receive any specific grant from funding agencies in the public, commercial, or not-for-profit sectors.

References

[1] J. Snelling, M.O. Barnett, D. Zhao, J.S. Arey, J. Air Waste Manag. Assoc. 56 (2006) 1484–1492.

[2] W. Piel, Preprints Symp. Oxygenates as Fuel Additives, 39 (1994) 273–281.

[3] M.A. Pérez, R. Bringué, M. Iborra, J. Tejero, F. Cunill, Appl. Catal. A Gen. 482 (2014) 38–48.

[4] B.H. Gwynn, J.H. Hirsch, US Patent 2 743 302 A, 1956.

[5] D. Gubisch, K. Armbrust, A. Kaizik, B. Scholz, R. Nehring, US Patent 6 015 928 A, 2000.

[6] T. Tsuchida, S. Sakuma, T. Takeguchi, W. Ueda, Ind. Eng. Chem. Res. 45 (2006) 8634–8642.

[7] P.H. Pfromm, V. Amanor-Boadu, R. Nelson, P. Vadlani, R. Madl, Biomass Bioenergy. 34 (2010) 515–524.

[8] F. Ancillotti, M. Massi Mauri, E. Pescarollo, J. Catal. 46 (1977) 49–57.

[9] R.S. Karinen, J.A. Linnekoski, A.O.I. Krause, Catal. Lett.76 (2001) 81–87.

[10] L.K. Rihko, J.A. Linnekoski, A.O.I. Krause, J. Chem. Eng. Data 39 (1994) 700–704.

[11] C. Gómez, F. Cunill, M. Iborra, F. Izquierdo, J. Tejero, Ind. Eng. Chem. Res. 36 (1997) 4756–4762.

[12] J.A. Linnekoski, A.O.I. Krause, A. Holmen, M. Kjetså, K. Moljord, Appl. Catal. A Gen. 174 (1998) 1–11.

[13] L. Solà, M.A. Pericàs, F. Cunill, J.F. Izquierdo, Ind. Eng. Chem. Res. 36 (1997) 2012–2018.

[14] O. Boonthamtirawuti, W. Kiatkittipong, A. Arpornwichanop, P. Praserthdam, S. Assabumrungrat, J. Ind. Eng. Chem. 15 (2009) 451-457.

[15] J. Guilera, L. Hanková, K. Jeřábek, E. Ramírez, J. Tejero, React. Funct. Polym. 78 (2014) 14–22.

[16] G.J. Hatchings, C.P. Nicolaides, M.S. Scurrell, Catal. Today 15 (1992) 23–49.

[17] J.L. Nocca, A. Forestierre, J. Cosyns, Fuel Reformul. 4 (1994) 18–22.

[18] C. Aellig, I. Hermans, ChemSusChem 5 (2012) 1737–1742.

[19] R. González, Performance of Amberlyst™ 35 in the synthesis of ETBE from ethanol and C_4 cuts, PhD Thesis, University of Barcelona, 2011.

[20] M. Iborra, J. Tejero, F. Cunill, J.F. Izquierdo, C. Fité, Ind. Eng. Chem. Res. 39 (2000) 1416–1422.

[21] F. Cunill, M. Vila, J.F. Izquierdo, M. Iborra, J. Tejero, Ind. Eng. Chem. Res. 32 (1993) 564–569.

[22] J.F. Izquierdo, F. Cunill, M. Vila, M. Iborra, J. Tejero, Ind. Eng. Chem. Res. 33 (1994) 2830–2835.

[23] M. Iborra, J. Tejero, M. Ben El-Fassi, F. Cunill, J.F. Izquierdo, C. Fité, Ind. Eng. Chem. Res. 41 (2002) 5359–5365.

[24] C. Fité, J. Tejero, M. Iborra, F. Cunill, J.. Izquierdo, D. Parra, Appl. Catal. A Gen. 169 (1998) 165–177.

[25] J. Tejero, F. Cunill, J.F. Izquierdo, M. Iborra, C. Fité, D. Parra, Appl. Catal. A Gen. 134 (1996) 21–36.

[26] J. Hidalgo, M. Zbuzek, R. Černý, P. Jíša, Open Chem. 12 (2014) 1–13.

[27] M. Vila, F. Cunill, J.-F. Izquierdo, J. González, A. Hernández, Appl. Catal. A Gen. 117 (1994) L99–L108.

[28] J. Tejero, a. Calderón, F. Cunill, J.F. Izquierdo, M. Iborra, React. Funct. Polym. 33 (1997) 201–209.

[29] J.H. Badia, C. Fité, R. Bringué, E. Ramírez, F. Cunill, Appl. Catal. A Gen. 468 (2013) 384–394.

[30] E.W. de Menezes, R. Cataluña, Fuel Process. Technol. 89 (2008) 1148–1152.

[31] C. Fité, M. Iborra, J. Tejero, J.F. Izquierdo, F. Cunill, Ind. Eng. Chem. Res. 33 (1994) 581–591.

[32] R.C. Reid, J.M. Prausnitz, B.E. Poling, The Properties of Gases and Liquids, fourth ed., McGraw-Hill, New York, 1987.

[33] B.E. Poling, J.M. Prausnitz, O. John Paul, R.C. Reid, The Properties of Gases and Liquids, fifth ed., McGraw-Hill, New York, 2001.

[34] C.L. Yaws, P.K. Narasimhan, in: C.L. Yaws (Ed.), Thermophysical Properties of Chemicals and Hydrocarbons, William Andrew, Norwich NY, 2009, pp. 672–682.

[35] R. Stewart, The proton: Applications to Organic Chemistry, Academic Press Inc., London, 1985.

[36] C. Buttersack, React. Polym. 10 (1989) 143–164.

[37] A. Chakrabarti, M.M. Sharma, React. Polym. 20 (1993) 1–45.

[38] J.F. Izquierdo, M. Vila, J. Tejero, F. Cunill, M. Iborra, Appl. Catal. A Gen. 106 (1993) 155–165.

[39] R.S. Karinen, A.O.I. Krause, Appl. Catal. A Gen. 188 (1999) 247–256.

[40] T. Matsuura, Synthetic Membranes and Membrane Separation Processes, CRC Press Inc., Boca Raton FL, 1993.

[41] C. Fité, J. Tejero, M. Iborra, F. Cunill, J.F. Izquierdo, AIChE J. 44 (1998) 2273–2279.

[42] C. Casas, R. Bringué, E. Ramírez, M. Iborra, J. Tejero, Appl. Catal. A Gen. 396 (2011) 129–139.

[43] J. Guilera, R. Bringué, E. Ramírez, M. Iborra, J. Tejero, Appl. Catal. A Gen. 413-414 (2012) 21–29.

[44] R. Bringué, E. Ramírez, M. Iborra, J. Tejero, F. Cunill, J. Catal. 304 (2013) 7–21.

[45] M.A. Tejero, E. Ramírez, C. Fité, J. Tejero, F. Cunill, Appl. Catal. A Gen. 517 (2016) 56–66.

[46] B. Corain, M. Zecca, K. Jeřábek, J. Mol. Catal. A Chem. 177 (2001) 3–20.

[47] K. Jeřábek, Anal. Chem. 57 (1985) 1598–1602.

[48] K. Jeřábek, Anal. Chem. 57 (1985) 1595–1597.

[49] T.N. Kwon, C. Jeon, J. Ind. Eng. Chem. 19 (2012) 68–72.

[50] S.M. Hosseini, S.S. Madaeni, A. Zendehnam, A.R. Moghadassi, A.R. Khodabakhshi, H. Sanaeepur, J. Ind. Eng. Chem. 19 (2013) 854–862.

[51] M. Umar, D. Patel, B. Saha, Chem. Eng. Sci. 64 (2009) 4424–4432.

[52] M.A. Harmer, Q. Sun, Appl. Catal. A Gen. 221 (2001) 45–62.

[53] U. Grömping, J. Stat. Softw. 17 (2006) 1-27.

[54] J.H. Badia, C. Fité, R. Bringué, M. Iborra, F. Cunill, Top. Catal. 58 (2015) 919–932.

FIGURES

Graphical abstract

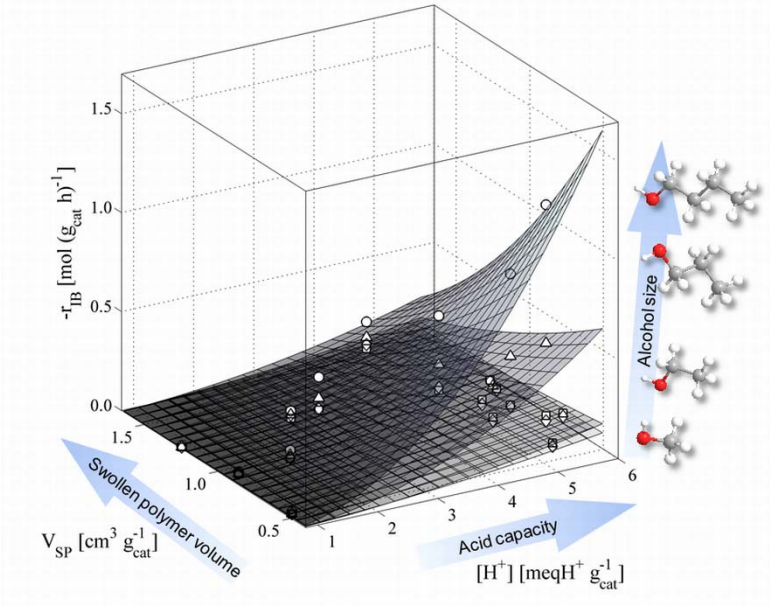

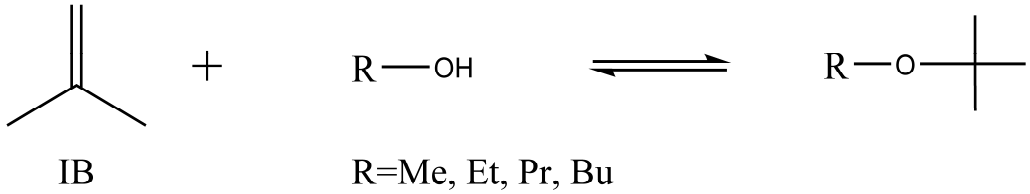

IB R=Me, Et, Pr, Bu

Figure 1. Studied etherification reactions

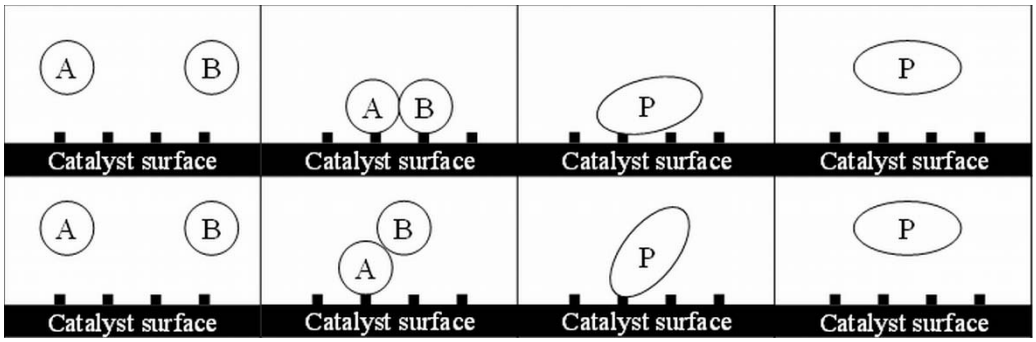

Figure 2. Reaction mechanisms

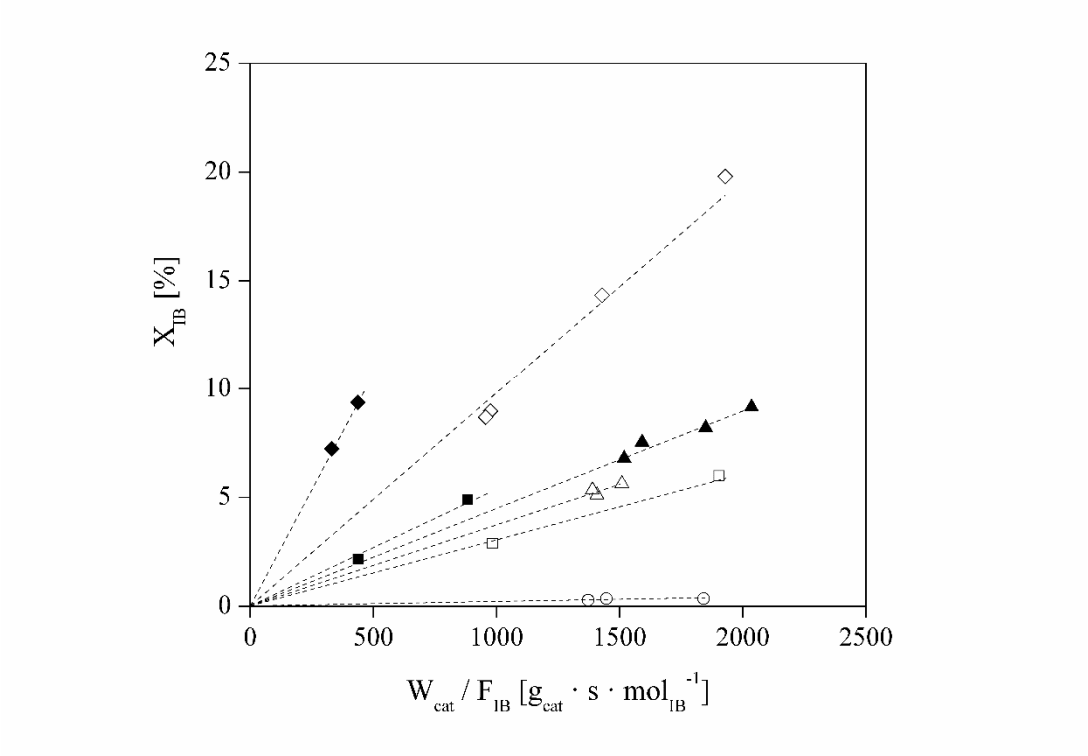

Figure 3. Experimental isobutene conversion for the studied reaction systems with different catalysts at 333 K and $R^{o}_{A/O}$ = 1.0. MTBE: A35 (Δ) and A46 (○); ETBE: A35 (▲); PTBE: CT275 (◊) and A39 (□); BTBE: CT275 (♦) and A39 (■)

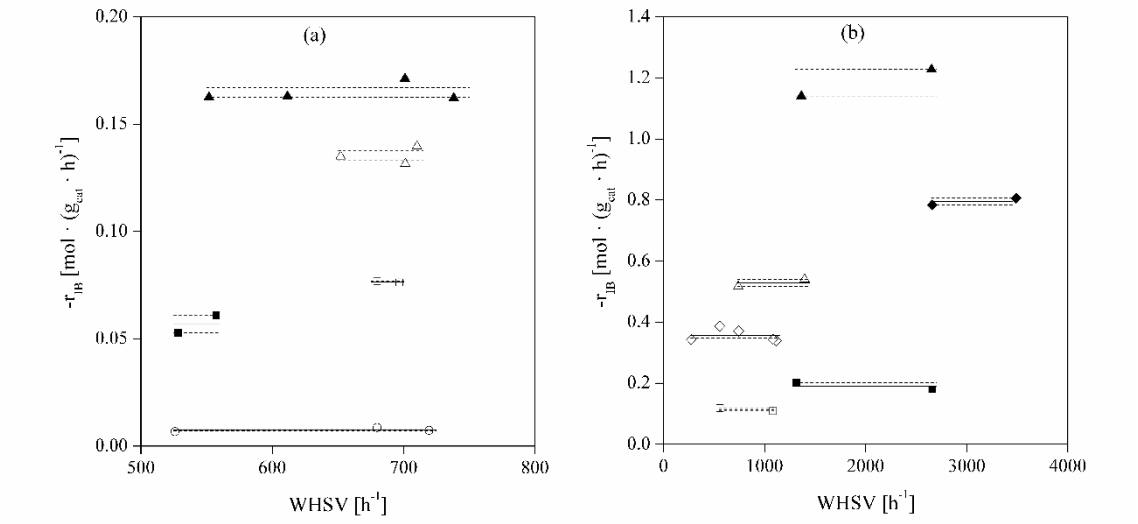

Figure 4. Influence of external mass transport on the rate at 333 K and $R^{o}_{A/O}$ = 1.0. (a) MTBE: A35 (Δ), A39 (□), A46 (○); ETBE: A35 (▲), A39 (■). (b) PTBE: A35 (Δ), CT275 (◊), A39 (□); BTBE: A35 (▲), CT275 (♦), A39 (■).——: mean value; - - -: standard error margin

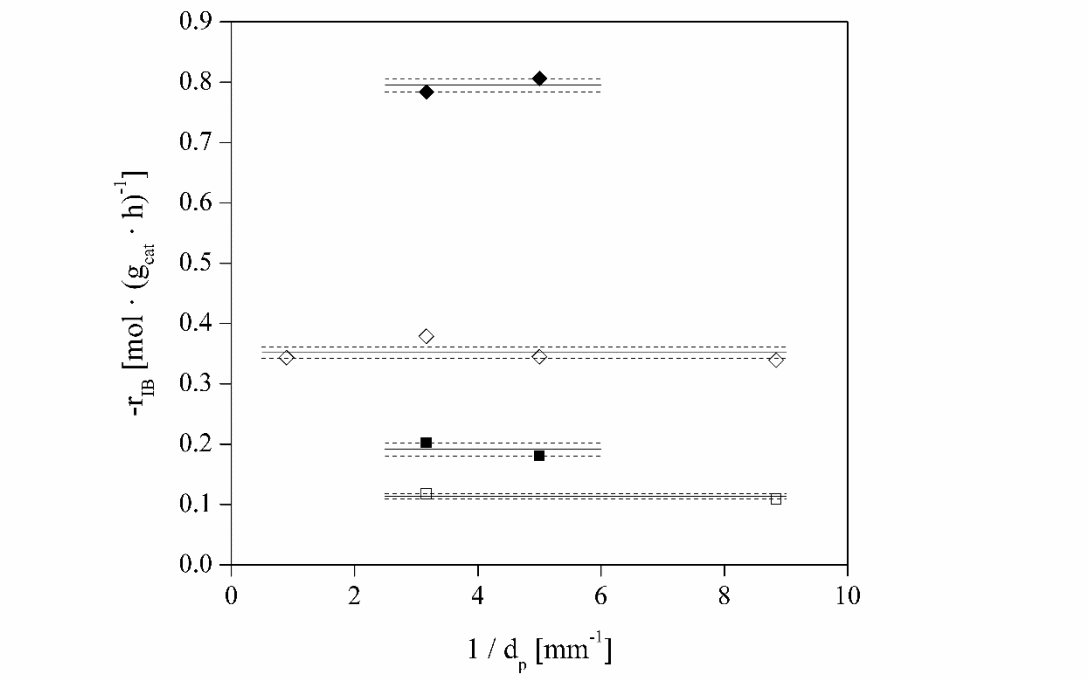

Figure 5. Influence of internal mass transport on the rate at 333 K and $R^{o}_{A/O}$ = 1.0. PTBE: CT275 (◊), A39 (□); BTBE: CT275 (♦) and A39 (■). (——: mean value; - - -: standard error margin)

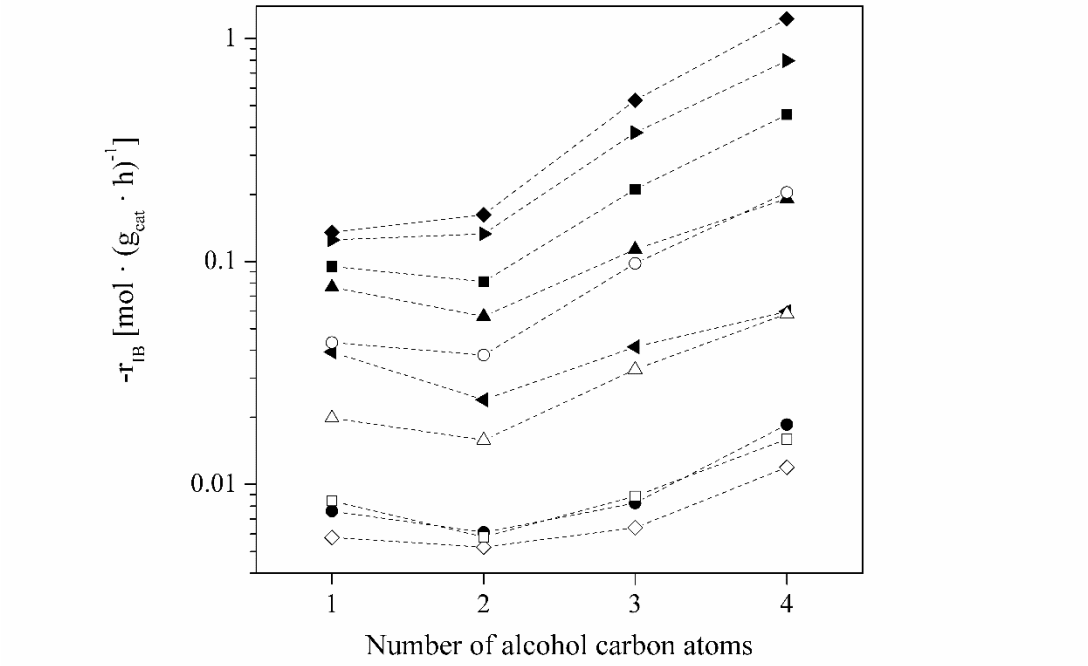

Figure 6. Isobutene reaction rate values for different catalysts versus alcohol number of carbon atoms. T = 333 K, $R^{o}_{A/O}$ = 1.0, d_p = 0.25-0.40 mm, WHSV > 500 h^{-1}. A16 (■), A35(♦), A39 (▲), A46 (●), A70 (◄), CT275 (►), 306 (◊), 406 (□), 606 (Δ), 806 (○)

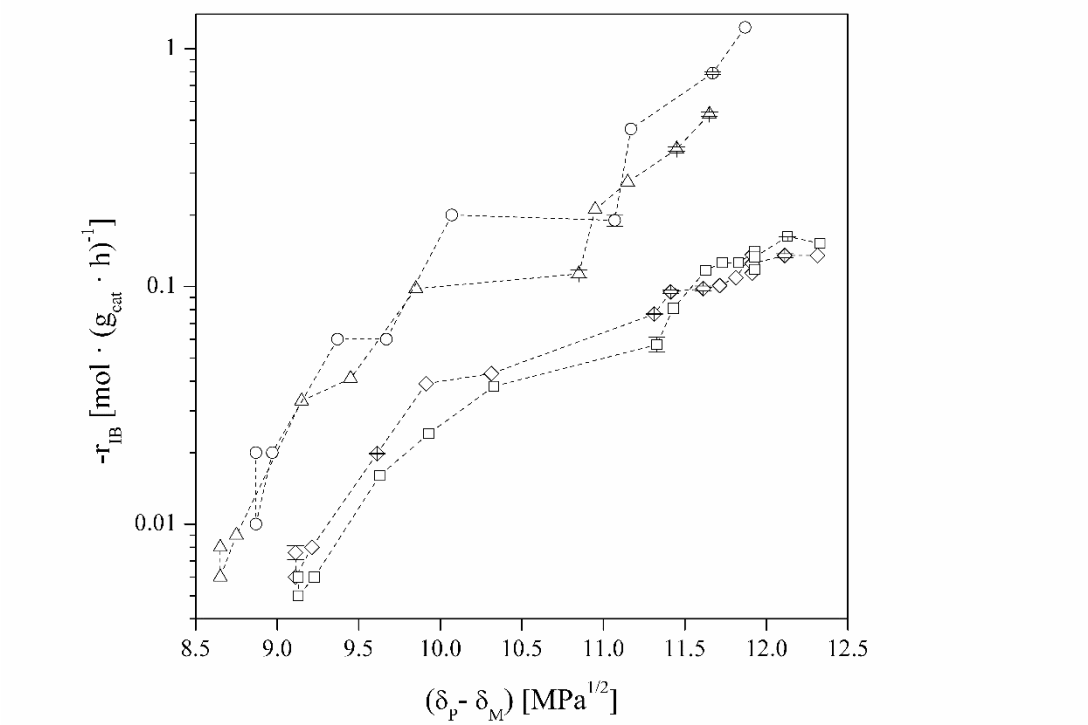

Figure 7. Isobutene reaction rate values for each synthesis reaction versus differences between the Hildebrand solubility parameter of the polymer, δ_P, and that of the medium, δ_M. T = 333 K, $R^o_{A/O}$ = 1.0, d_p = 0.25-0.40 mm, WHSV > 500 h^{-1}. MTBE (◊), ETBE (□), PTBE (Δ), BTBE (○)

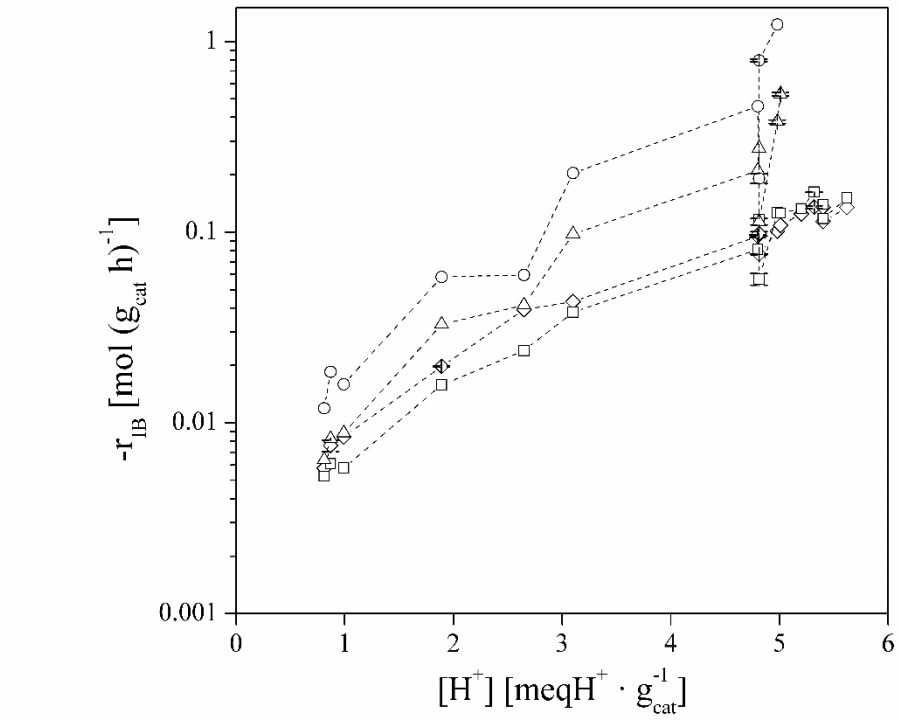

Figure 8. Effect of the catalysts acid capacity on the reaction rate. T = 333 K, $R^o_{A/O}$ = 1.0, d_p = 0.25-0.40 mm, WHSV > 500 h^{-1}. MTBE (◊), ETBE (□), PTBE (Δ), BTBE (○)

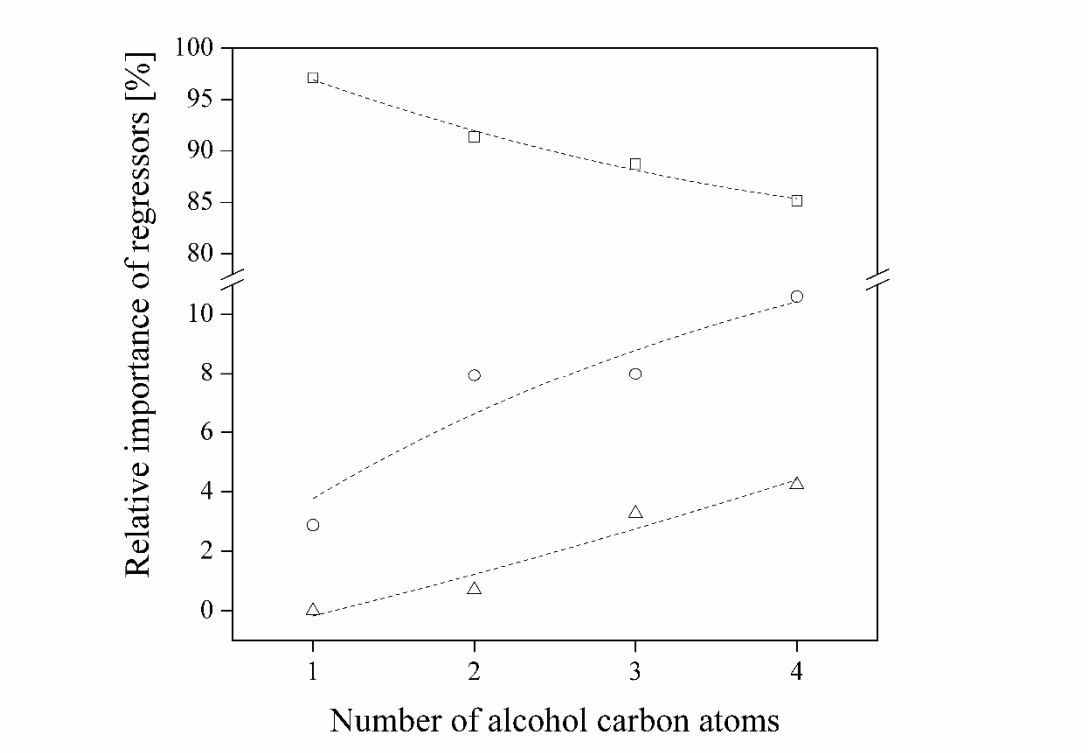

Figure 9. Relative importance of regressors versus alcohol number of carbon atoms. $[H^+]$ (□), V_{sp} (○) and $[H^+]\cdot V_{sp}$ (Δ)

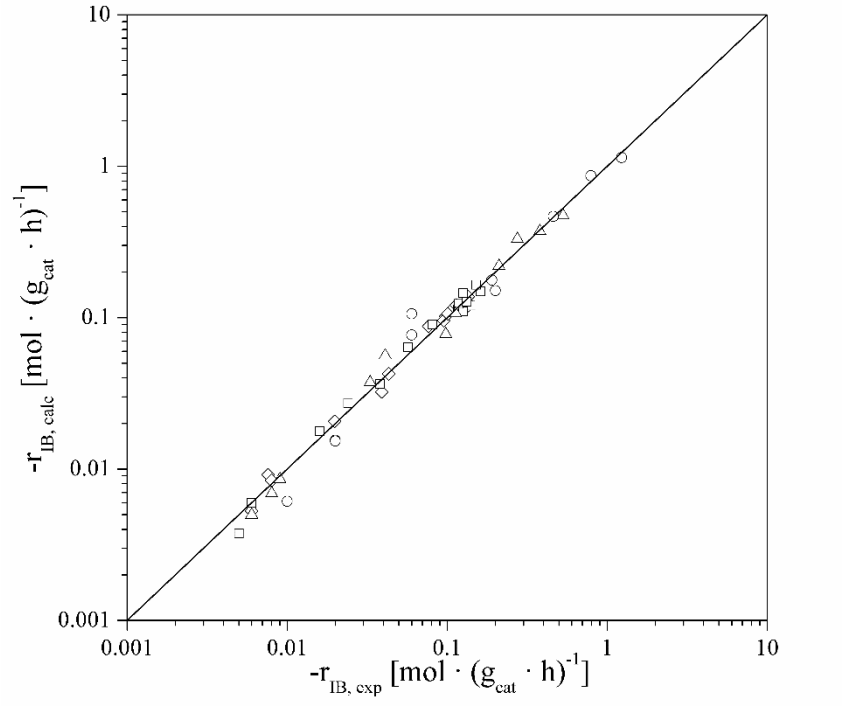

Figure 10. Reaction rate fit for the considered reactions. T = 333 K, $R°_{A/O}$ = 1.0, d_p = 0.25-0.40 mm, WHSV > 500 h^{-1}. MTBE (◊), ETBE (□), PTBE (Δ) and BTBE (○)

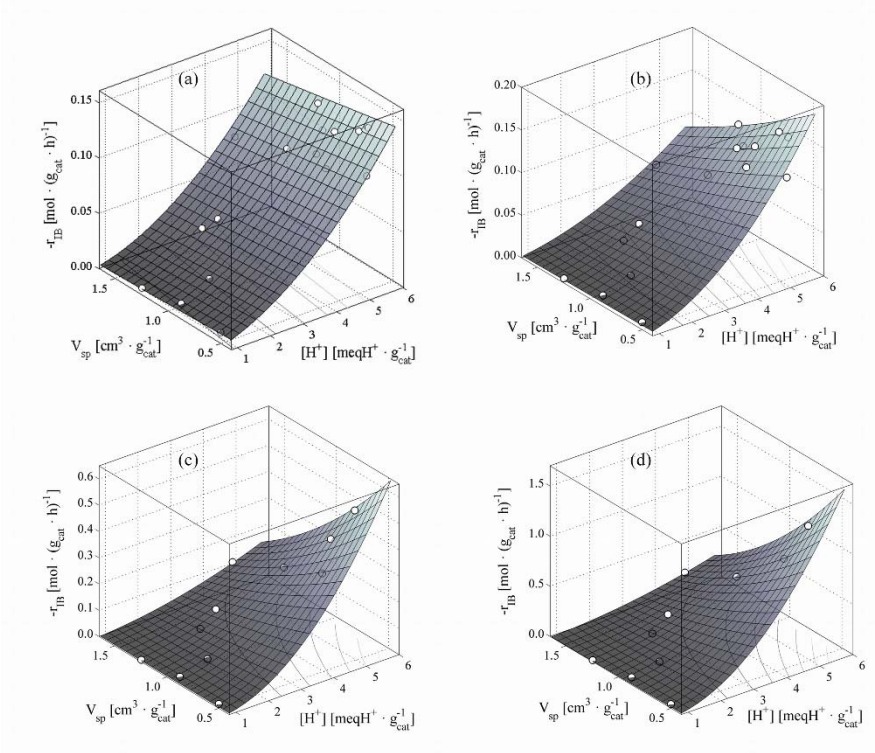

Figure 11. Response surfaces for the syntheses of (a) MTBE, (b) ETBE, (c) PTBE, and (d) BTBE

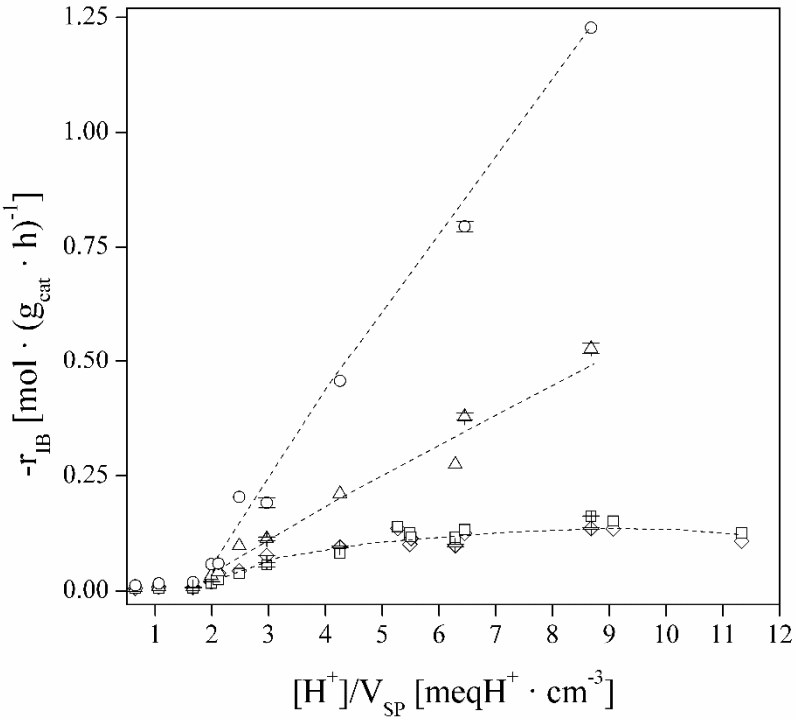

Figure 12. Effect of the $[H^+]/V_{sp}$ ratio on the etherification rate. T = 333 K, $R^o_{A/O}$ = 1.0, d_p = 0.25-0.40 mm, WHSV > 500 h^{-1}. MTBE (◊), ETBE (□), PTBE (Δ) and BTBE (○)